

# FORMATION OF A $33 M_{\odot}$ BLACK HOLE IN A LOW-METALLICITY BINARY

KAREEM EL-BADRY<sup>1</sup>

<sup>1</sup>Department of Astronomy, California Institute of Technology, 1200 E. California Blvd., Pasadena, CA 91125, USA  
Version April 22, 2024

## ABSTRACT

A  $33 M_{\odot}$  black hole (BH) was recently discovered in an 11.6-year binary only 590 pc from the Sun. The system, Gaia BH3, contains a  $0.8 M_{\odot}$  low-metallicity giant ( $[M/H] = -2.2$ ) and is kinematically part of the Galactic halo, suggesting that the BH formed from a low-metallicity massive star. I show that orbits similar to that of Gaia BH3 are naturally produced through isolated binary evolution. The system's period and eccentricity can result from a broad range of initial orbits with a modest natal kick ( $v_{\text{kick}} \lesssim 75 \text{ km s}^{-1}$ ) to the BH. I construct MESA models for metal-poor massive stars with initial masses ranging from  $35 - 55 M_{\odot}$ , which reach maximum radii of  $1150 - 1800 R_{\odot}$  as red supergiants. Stars of this size would fit inside most plausible pre-supernova orbits for the system without overflowing their Roche lobes. In addition, models with moderately rapid initial rotation ( $\Omega/\Omega_{\text{crit}} \gtrsim 0.45$ ) undergo chemically homogeneous evolution and never expand to radii larger than  $10 R_{\odot}$ . There are thus multiple channels through which a low-metallicity, extreme-mass ratio binary could produce a system like Gaia BH3. Dynamical formation scenarios are also viable, and there is little doubt that both isolated and dynamically-formed BH binaries with orbits similar to Gaia BH3 will be discovered in Gaia DR4. Only about 1 in 10,000 stars in the solar neighborhood have metallicities as low as Gaia BH3. This suggests that BH companions are dramatically over-represented at low-metallicity, though caveats related to small number statistics apply. The fact that the luminous star in Gaia BH3 has been a giant — greatly boosting its detectability — only for  $\sim 1\%$  of the time since the system's formation implies that additional massive BHs remain to be discovered with only moderately fainter companions.

*Subject headings:* stars: black holes – stars: massive – stars: evolution – supergiants

## 1. INTRODUCTION

Gaia Collaboration et al. (2024) recently reported discovery of an astrometric binary containing a  $0.8 M_{\odot}$  star on the lower giant branch and a  $33 M_{\odot}$  dark companion that is presumably a black hole (BH). The system, which they named Gaia BH3, was discovered with pre-release DR4 astrometry, and its orbital motion was confirmed with (nearly) independent radial velocity measurements from the *Gaia* RVS spectrometer.

The discovery is exciting for several reasons. First, Gaia BH3 contains the most massive robustly measured stellar-mass BH in the local Universe. Second, the star has the lowest metallicity of any known star orbiting a BH,  $[M/H] = -2.2$ . Third, the system provides the first empirical evidence that low-metallicity massive stars leave behind massive BHs, making them prime candidates for being progenitors of gravitational wave sources. And fourth, the system is bright and nearby ( $G = 11.2$ ,  $d = 590$  pc), suggesting that many similar systems that are fainter and/or more distant remain to be discovered.

Gaia BH3 is the widest BH binary discovered to date, with an orbital period of  $\sim 4250$  days and a semimajor axis of  $\sim 16.5$  au. The eccentricity is relatively high,  $e \approx 0.73$ , such that the star and BH pass within 4.5 au of each other at periastron. How the system formed is uncertain. Gaia Collaboration et al. (2024) note that a typical red supergiant would not fit within the current orbit at periastron. They thus consider formation of the

system from an isolated binary unlikely, and invoke dynamical exchange as a possible alternative.

Here, I consider the possibility of formation from an isolated binary in more detail. I conclude that — although dynamical formation channels are also viable — Gaia BH3's properties may be naturally explained as the end state of an isolated, extreme mass ratio binary. The main differences between my analysis and that of Gaia Collaboration et al. (2024) are that (a) I consider the possibility that the orbit today may be different from the orbit at the time of the BH's formation, due to kicks and/or mass loss during the BH progenitor's death, and (b) I show that low-metallicity massive stars remain compact for most of their evolution, expanding to red supergiant dimensions only in the final  $\sim 1000$  years of their lives, if at all. As a result, there is a broad parameter space of initial orbits in which the BH progenitor either never fills its Roche lobe, or fills it too late for the companion star to spiral inward significantly.

The remainder of this paper is organized as follows. Section 2 uses Monte Carlo simulations of BH formation to assess the likely initial separation if Gaia BH3 formed from an isolated binary. In Section 3, I describe evolutionary models for low-metallicity massive stars that could form the BH. Section 4 argues that BH companions appear to be strongly overrepresented at low metallicity, and that additional nearby BHs orbited by low-metallicity stars likely remain to be discovered. Future prospects and broader implications are briefly discussed in Section 5.

## 2. CONSTRAINTS ON THE PROGENITOR ORBIT

I use Monte Carlo simulations to study the combinations of pre-supernova<sup>1</sup> (SN) orbits and natal kicks that could have produced an orbit similar to that of Gaia BH3. This approach follows Tauris et al. (2017) and El-Badry et al. (2024); see Tauris & van den Heuvel (2023) for additional details about SN kicks. In brief, I simulate a large number ( $N = 10^7$ ) of orbits and kicks, and then use the formalism from Brandt & Podsiadlowski (1995) to predict the post-SN parameters. Finally, I analyze the initial parameters of the simulations for which the final period and eccentricity are close to the observed values for Gaia BH3:  $P_{\text{orb,final}} = 4000 - 4500$  d, and  $e_{\text{final}} = 0.68 - 0.78$ . Narrowing these ranges reduces the number of surviving Monte Carlo samples but has no significant effect on their distribution.

I begin with a uniform distribution of pre-SN orbital periods between 0 and 8500 d (twice the currently observed orbital period of Gaia BH3). I simulate kicks assuming orientations distributed uniformly on the sky and velocities distributed uniformly between 0 and  $100 \text{ km s}^{-1}$ . I take a uniform distribution of  $\Delta m$ , the mass loss of the BH progenitor during the SN, between 0 and  $20 M_{\odot}$ , implying a progenitor mass of  $33\text{--}53 M_{\odot}$ . I assume the pre-SN orbit had  $e = 0$ , having been circularized by tides when the BH progenitor expanded. This is not a population synthesis simulation – pre-SN orbits are unlikely to be uniformly distributed in all parameters – but should be viewed as an exploration of what combinations of orbits, kicks, and mass loss could have produced the observed orbit. Later, I will check whether the possible progenitor orbits are consistent with the expected size of the BH progenitor as a red supergiant. If not – or if an orbit similar to the observed one could only be produced self-consistently from very fine-tuned initial conditions – this would suggest that formation from an isolated binary is unlikely.

The results of this experiment are shown in Figure 1. Initial separations ranging from  $\sim 800$  to  $\sim 6000 R_{\odot}$  can produce the observed orbit. Initial separation closer than  $\sim 800 R_{\odot}$  cannot, because widening these to the separation observed today via a kick or mass loss would result in a higher final eccentricity than is observed. Wider initial separations *could* match the orbit for suitably chosen kicks, but these are excluded by our prior of  $P_{\text{orb,init}} < 8500$  d. The median and middle 68% range of pre-SN separations that reproduce the observed orbit is  $a_{\text{init}} = 4473_{-2146}^{+1347} R_{\odot}$ ; this range encompasses the semimajor axis observed today, which is  $\approx 3350 R_{\odot}$ .

A broad range of  $v_{\text{kick}}$  can also reproduce the observed orbit; I find a middle 68% range of  $v_{\text{kick}} = 39_{-14}^{+19} \text{ km s}^{-1}$ . There is no strong correlation between the allowed  $v_{\text{kick}}$  and  $a_{\text{init}}$ , but the combination of low  $v_{\text{kick}}$  ( $\lesssim 20 \text{ km s}^{-1}$ ) and large initial separation ( $\gtrsim 1200 R_{\odot}$ ) is ruled out because such orbits produce too low eccentricities. The pre-SN mass is not strongly constrained. Only for  $M_{2,\text{init}} > 67 M_{\odot}$  (where most orbits become unbound due to Blaauw 1961 kicks) would this parameter strongly affect the results. In the limit of  $M_{2,\text{init}} = 33 M_{\odot}$  (no mass loss), the required initial separation to explain the

orbit decreases slightly, to  $a_{\text{init}} = 4010_{-2539}^{+1314} R_{\odot}$ .

Assuming the system formed from an isolated binary and the orbit was affected by a natal kick, we can ask whether significant fine-tuning is required to explain the orbit. Fine-tuning is always required to produce any *specific* orbit; here I am concerned with whether the orbit of Gaia BH3 is typical of the predicted BH + main sequence star population, given the inferred kick velocities. If I fix  $v_{\text{kick}} = 39 \text{ km s}^{-1}$  and repeat the experiment, I find that  $\approx 50\%$  of all simulated orbits remain bound, and the median eccentricity of the orbits that remain bound is 0.68. This suggests that Gaia BH3 is typical of the predicted population and the orbit does not require much fine-tuning to explain. If  $v_{\text{kick}}$  is increased to  $80 \text{ km s}^{-1}$ , the fraction of orbits that remain bound falls to 20%.

The largest star that could fit inside a pre-SN orbit of semimajor axis  $a_{\text{init}}$  has radius  $R_{\text{max}} = a_{\text{init}} f_q$ , where  $f_q(M_1/M_2)$  is given by Eggleton (1983) and varies from 0.68 to 0.70 over  $M_1 = 35 - 50 M_{\odot}$ , assuming  $M_2 = 0.8 M_{\odot}$ . This means for the pre-SN orbits that reproduce the observed period and eccentricity, the  $\pm 1\sigma$  range of maximum radii is  $R_{\text{max}} \approx 3090_{-2170}^{+930} R_{\odot}$ . We are now in a position to ask whether the progenitor of the BH, which was presumably a low-metallicity massive star, would have fit inside the pre-SN orbit.

## 3. THE BH PROGENITOR

I calculated a small suite of evolutionary models for the progenitor of the BH using MESA (Paxton et al. 2011, 2013, 2015, 2018, 2019; Jermyn et al. 2023). The calculations closely follow the setup described by Klencki et al. (2020), with MESA updated to version r23.05.1. The most important ingredients are summarized below, and I refer to Klencki et al. (2020, 2021) for more details.

I evolve single stars with initial masses ranging from  $30$  to  $55 M_{\odot}$  and metallicities ranging from  $Z = 0.00002$  ( $[M/H] = -2.8$ ) to  $Z = 0.0014$  ( $[M/H] = -1.0$ ). Convection is modeled following Henyey et al. (1965) (`mlt_option` = ‘Henyey’) with a default mixing length parameter  $\alpha = 1.5$ . The Ledoux criterion is used and semiconvection is modeled following Langer et al. (1983), with efficiency parameter  $\alpha_{\text{SC}} = 100$  motivated by Schootemeijer et al. (2019). MLT++ is not used. Step overshooting is assumed above the H and He burning cores, with `overshoot_f` = 0.33 and `overshoot_f0` = 0.05 by default. I experiment with varying the mixing length and overshooting parameter, as described below.

Stellar winds are modeled following Brott et al. (2011): for hot, hydrogen-rich stars ( $T_{\text{eff}} > 25 \text{ kK}$ ;  $X_S > 0.7$ ), the models take the wind mass loss rates from Vink et al. (2000, 2001, here  $X_S$  is the surface hydrogen mass fraction). For hydrogen-poor stars ( $X_S < 0.4$ ), they use the Wolf-Rayet wind model from Hamann et al. (1995) and reduce the mass loss rate by a factor of 10 to account for wind clumping (Yoon et al. 2006). For stars with intermediate surface hydrogen abundances ( $0.4 < X_S < 0.7$ ), the mass loss rate is interpolated between the two prescriptions above. For stars cooler than  $T_{\text{eff}} = 25 \text{ kK}$ , the mass loss rate is set to the larger of the rates predicted by Nieuwenhuijzen & de Jager (1990) and Vink et al. (2001). These mass loss rates all include a  $\dot{M} \propto Z^{0.85}$  scaling with metallicity. As a result, the predicted wind mass-loss rates are all rather low at the metallicities of

<sup>1</sup> Here “supernova” loosely refers to the death of the massive star and formation of the BH. Whether there was a successful explosion or a long-lived luminous transient is uncertain.

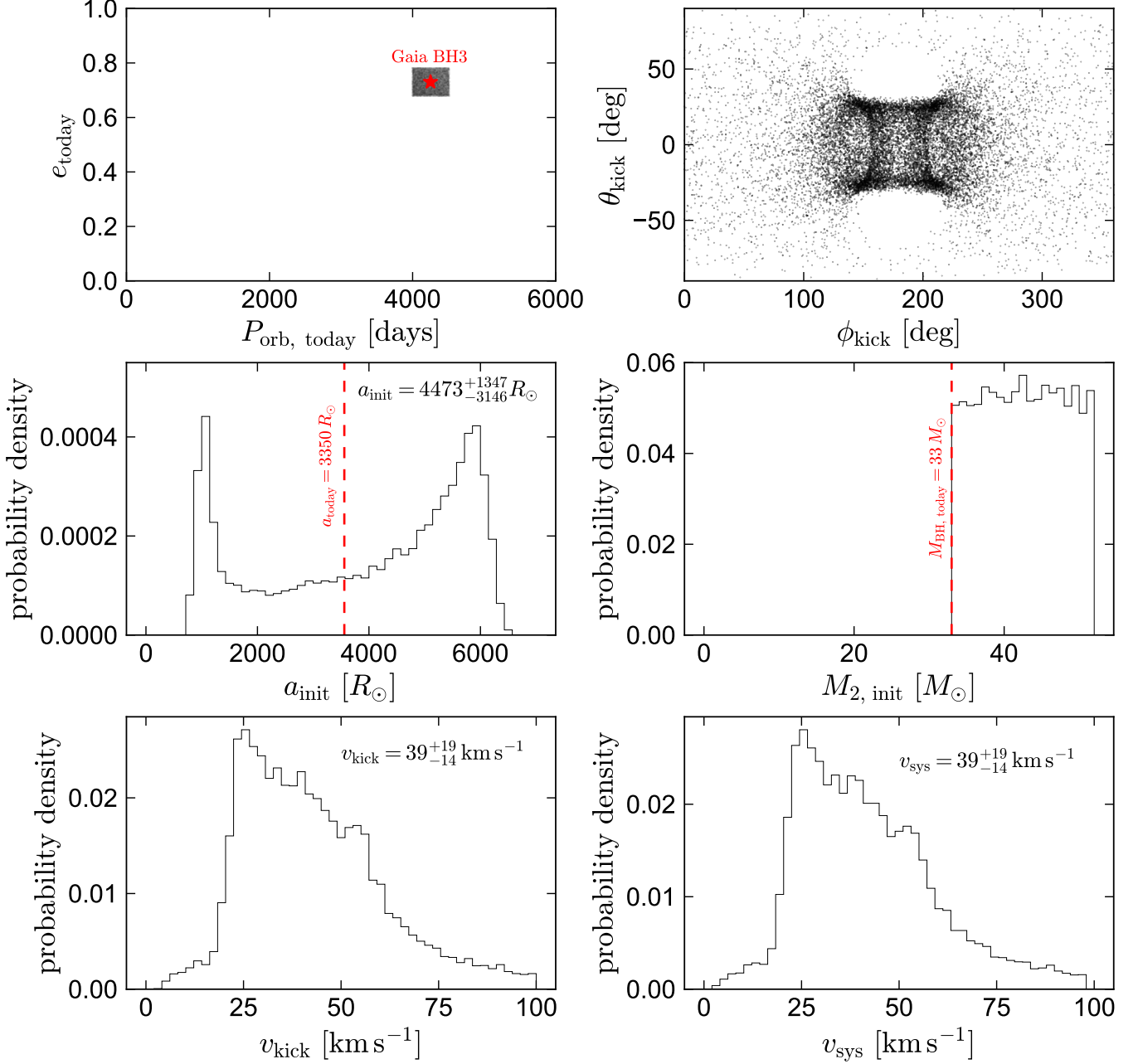


FIG. 1.— Constraints on kicks and the pre-SN orbit of Gaia BH3-like binaries. I assume that the binary had a circular orbit before the SN and that the BH received a kick with velocity  $v_{\text{kick}}$  when it formed. I simulate  $10^7$  pre-SN orbits with a uniform period distribution  $P_{\text{orb}} \sim \mathcal{U}(0, 2P_{\text{orb, BH3}})$ , a pre-SN mass distribution  $M_{2, \text{init}}/M_{\odot} \sim \mathcal{U}(33, 53)$ , and a kick velocity distribution  $v_{\text{kick}}/(\text{km s}^{-1}) \sim \mathcal{U}(0, 100)$ . I then show properties of the systems whose post-SN orbits have periods and eccentricities similar to Gaia BH3 (upper left). These orbits have a wide range of pre-SN separations, ranging from 1000 to 6000  $R_{\odot}$ .

interest for Gaia BH3. For consistency with Klencki et al. (2020), the models assume  $Z_{\odot} = 0.017$  when calculating mass loss rates, but I label the metallicities by  $[M/H] = \log(Z/0.014)$  following Asplund et al. (2009).

For rotating models, I include the effects of Eddington-Sweet circulation (`D_ES_factor` = 1.0), secular shear instabilities (`D_SSI_factor` = 1.0), and the Goldreich-Schubert-Fricke instability (`D_GSF_factor` = 1.0), with an efficiency factor `am_D_mix_factor` = 1/30 following Heger et al. (2000). I initialize models using the MESA `create_pre_main_sequence_model` routine and run un-

til the end of carbon burning, by which time the model is within days of core collapse and there is no time for further radius evolution. I limit the timestep with `varcontrol.target` = 0.0001 and `delta_HR_limit` = 0.0005 and the mesh resolution with `max_dq` = 0.001. Sensitivity to these choices was explored by Klencki et al. (2021).

To verify that the problem setup is consistent with the one used by Klencki et al. (2020), I began by reproducing their 35  $M_{\odot}$  at metallicity  $Z = 0.00017$  and comparing to their published tracks. The model reaches a maximum

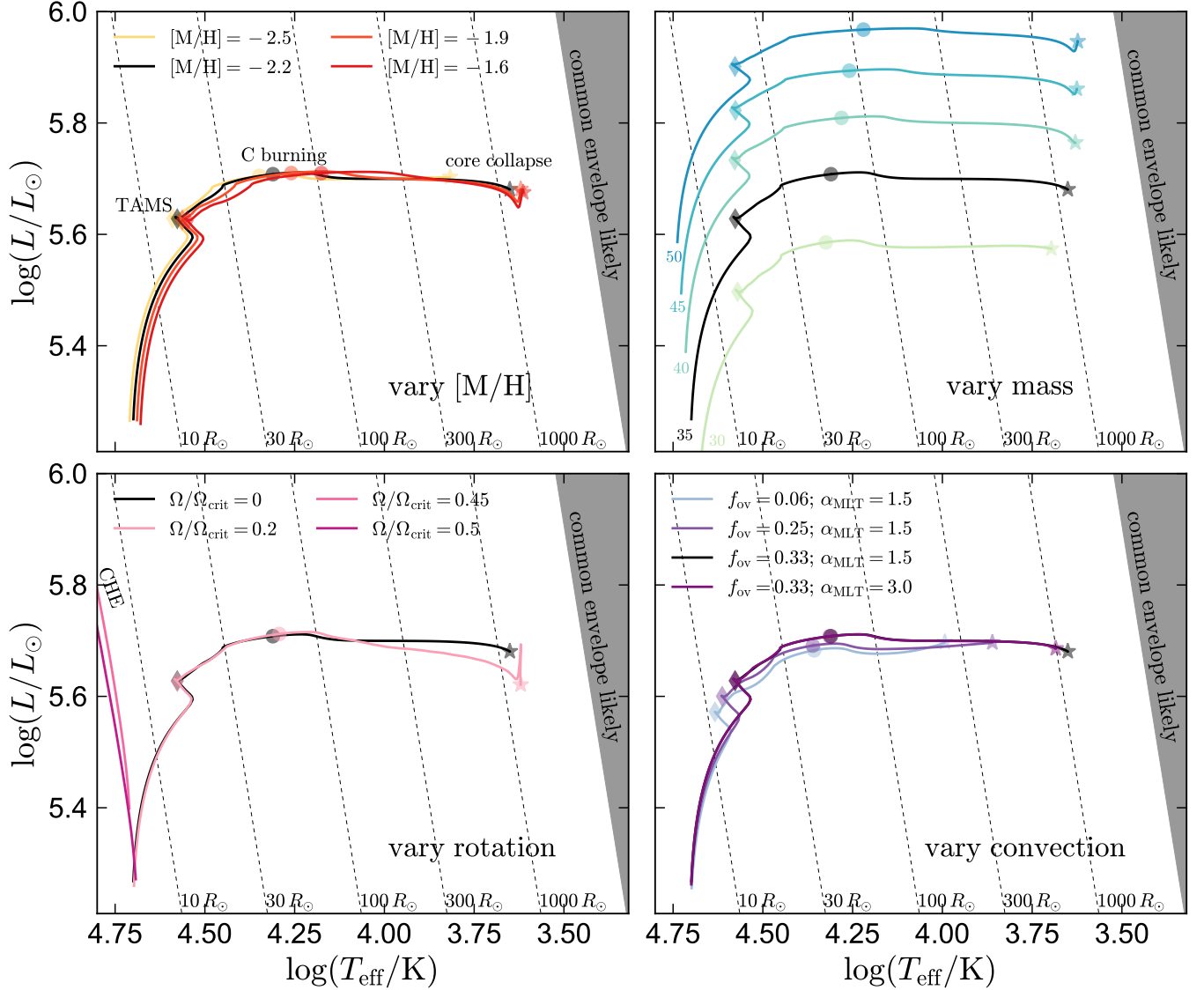


FIG. 2.— MESA evolutionary models for low-metallicity massive stars. The model shown in black is the same in all three panels: a  $35 M_{\odot}$  star with metallicity  $[M/H] = -2.2$  and no rotation. Colored lines show models varying metallicity (upper left), initial mass (upper right), initial rotation rate (lower left), and overshooting or mixing length (lower right). Diamonds, circles, and stars mark core hydrogen exhaustion, the onset of carbon burning, and core collapse. Dashed diagonal lines show constant radius. Shaded gray region marks  $R > 3000 R_{\odot}$ , beyond which the star would have been unlikely to fit inside the pre-SN orbit of Gaia BH3. All of the models avoid this limit, and some remain much smaller than it, such that they would not overflow their Roche lobes for any plausible progenitor orbit of Gaia BH3. Lower left highlights models undergoing chemically homogeneous evolution (CHE), which stay smaller than  $10 R_{\odot}$  at this metallicity, even for modest initial rotation rates,  $\Omega/\Omega_{\text{crit}} \gtrsim 0.45$ . CHE represents one possible channel to form Gaia BH3, but even models without rotation could quite plausibly fit within the pre-SN orbit.

radius of  $1331 R_{\odot}$  shortly before core collapse. Their corresponding track has a maximum radius  $1340 R_{\odot}$  at the same point, and its evolution in the HR diagram is nearly indistinguishable from that of the model calculated here.

Figure 2 shows the evolution of several models in the HR diagram. Core hydrogen exhaustion, the onset of carbon burning, and the end of carbon burning are marked in each panel with a diamond, circle, and star symbol, respectively. As a fiducial model – shown in black in each panel – I take the nonrotating model with initial mass of  $35 M_{\odot}$  and metallicity  $[M/H] = -2.2$ . The mass of this model at the end of carbon burning is  $34.7 M_{\odot}$ , reflecting the fact that winds are predicted to be very weak at these metallicities. This model could be expected to produce

a  $\sim 33 M_{\odot}$  BH if the SN shock fails and it undergoes core collapse with little mass loss, since loss of up to a few  $M_{\odot}$  is still expected to occur as a result of neutrino mass loss and the subsequent shock (Fernández et al. 2018). The fiducial model reaches a maximum radius of  $1150 R_{\odot}$  shortly before core collapse.

The four panels in Figure 2 show the effects of varying metallicity, mass, rotation, and convective mixing length and overshooting. The maximum radius reached by our models varies relatively weakly with metallicity over  $-2.2 < [M/H] < -1.6$ . The model with  $[M/H] = -2.5$  (slightly lower than Gaia BH3) is significantly smaller than other models, reaching a maximum radius of  $\sim 550 R_{\odot}$ . The maximum radius increases with



initial mass, ranging from  $\approx 850 R_{\odot}$  for the  $30 M_{\odot}$  model to  $\approx 1800 R_{\odot}$  for the  $50 M_{\odot}$  model at  $[M/H] = -2.2$ . The maximum radius is sensitive to overshooting, as explored by Schootemeijer et al. (2019): smaller overshooting parameters lead to more compact supergiants. For the choice of parameters explored here, sensitivity to the mixing length is relatively weak: increasing  $\alpha_{\text{MLT}}$  from 1.5 to 3.0 reduces the maximum radius by  $\sim 10\%$ .

All the models shown in Figure 2 are consistent with fitting within the observed orbit for more than half of the sampled initial separations: the shaded regions in Figure 2 show  $R > 3000 R_{\odot}$ , above which stars would overflow their Roche lobes in Gaia BH3 for about half of the possible initial orbits shown in Figure 1. None of the models reach radii of  $3000 R_{\odot}$ , implying that they would not overflow their Roche lobes for a majority of the possible pre-SN orbits.

One of the main differences between these and higher-metallicity models is that these models remain compact during core He burning: although they are red supergiants at the end of their lives, they spend the large majority of their post-main sequence evolution as blue or yellow supergiants with  $R \lesssim 100 R_{\odot}$ , and only expand to red supergiant dimensions during their final  $\sim 1000$  years (see Klencki et al. 2020, for further discussion). This is illustrated in Figure 3, which shows the late-stage radius evolution for models with a range of masses (top panel) and metallicities (bottom panel). The fiducial model increases its radius by a factor of 2 in its final 800 years. This behavior is not found in higher metallicity models, even at “low” metallicities comparable to those found in the Magellanic clouds. The upshot is that if a star with properties similar to those predicted by the MESA models overflowed its Roche lobe in the Gaia BH3 system, it would only have done so in the final few hundred years of its evolution.

If a red supergiant overflows its Roche lobe, the inspiral of the companion star is not instantaneous, but occurs only once the work done by the drag force is comparable to the star’s orbital energy. For the large mass ratios and diffuse envelopes of interest here, the expected inspiral time from the outer envelope is of order  $10^2$  orbits (O’Connor et al. 2023), or of order  $10^3$  years. Since most of our models expand significantly in their final  $\sim 1000$  years, it is possible that the BH progenitor *did* overflow its Roche lobe, but then collapsed soon after, not leaving the companion star enough time to spiral in. Such an evolutionary history is most likely to be tenable for pre-SN orbits in which the BH progenitor just barely overflows its Roche lobe.

The lower left panel of Figure 2 shows another possible formation channel: formation from a rapidly-rotating star through chemically homogeneous evolution (CHE). At high rotation rates, large-scale meridional circulations efficiently mix helium into the envelope, preventing the buildup of a chemical gradient and core/envelope dichotomy that leads to expansion in nonrotating models (Maeder 1987; Yoon & Langer 2005; Woosley & Heger 2006). Under CHE, stars evolve from the main sequence toward the helium main sequence, where they have effective temperatures above  $10^5$  K and radii smaller than  $1 R_{\odot}$ . These models eventually ignite carbon burning and terminate their evolution without ever reaching  $R > 10 R_{\odot}$ . At the low metallicities considered

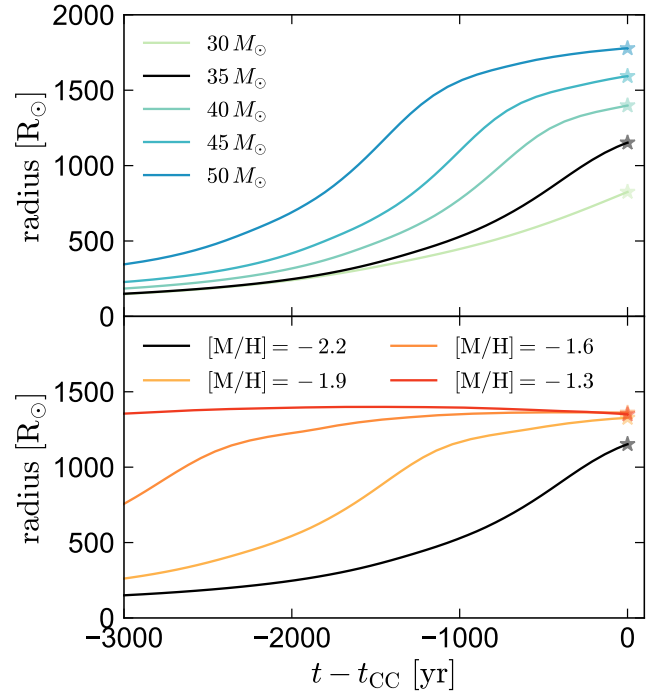


FIG. 3.— Radius evolution of MESA models in the final years before core collapse. Mass is varied in the top panel, and metallicity in the bottom panel. At low metallicity, the models expand significantly in the final  $\sim 1000$  yr of their evolution, only appearing as red supergiants shortly before core collapse. Expansion occurs earlier at higher metallicity. If the fiducial model (black) were put in an orbit in which it overflowed its Roche lobe at  $R = 1000 R_{\odot}$ , this would occur only a few tens of orbits before core collapse, giving the companion insufficient time to spiral inward very far.

here, CHE occurs with modest initial rotation rates,  $\Omega/\Omega_{\text{crit}} \geq 0.45$ .

#### 4. POPULATION INFERENCE FROM $N = 1$

##### 4.1. Wide BH companions are overrepresented at low metallicity

Gaia BH3 has a much lower metallicity than typical stars in the solar neighborhood. It is expected that low-metallicity massive stars may form higher-mass BHs due to their weaker winds (Woosley et al. 2002), and Gaia BH3 was published in advance of DR4 primarily because of the BH’s high mass. However, I argue here that – even ignoring the BH’s mass – the fact that a BH of any mass was found with such a low-metallicity companion suggests that wide BH companions are overrepresented at low metallicity.

Figure 4 shows differential and cumulative metallicity distributions of giants within 1 kpc of the Sun. In black, I show giants with high-quality metallicities from Gaia XP spectra, which I take from Table 2 of Andrae et al. (2023). In red, I show giants with high-SNR spectra from DR 17 of the APOGEE survey (Majewski et al. 2017; Abdurro’uf et al. 2022). Here I exclude stars targeted non-randomly, since several of the APOGEE targeting cartons intentionally selected low-metallicity stars. The shaded gray region shows the plausible metallicity uncertainty of Gaia BH3, which goes from  $[M/H] = -2.2$  as estimated by Gaia Collaboration et al. (2024) to  $[M/H] = -1.82$  as estimated for the source by Andrae et al. (2023). I assume  $[M/H] = -2.0$  in the discussion

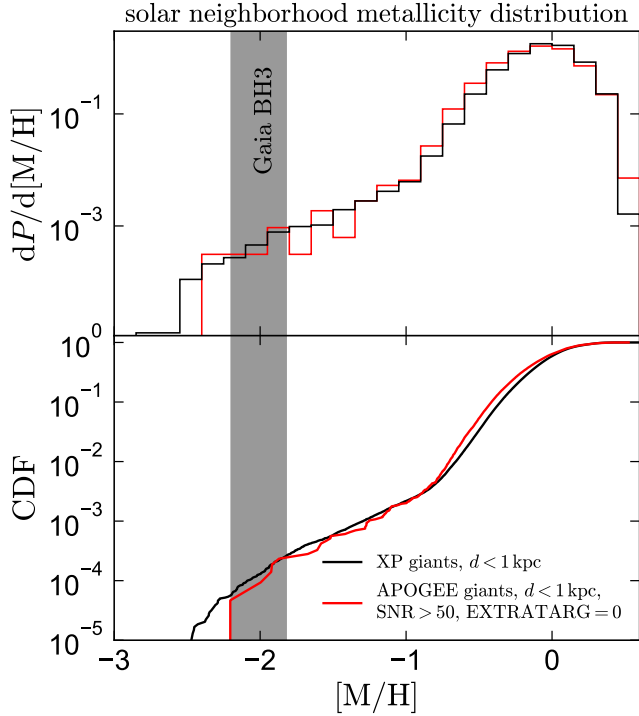


FIG. 4.— Metallicity distribution of red giants within 1 kpc of the Sun, calculated from the *Gaia* XP metallicity catalog of Andrae et al. (2023, black) and APOGEE DR17 (Abdurro’uf et al. 2022, red). The metallicity of Gaia BH3 is marked with a shaded region:  $[M/H] = -1.82$  according to Andrae et al. (2023), and  $[M/H] = -2.2$  according to Gaia Collaboration et al. (2024). The fraction of giants with metallicities as low as Gaia BH1 is only  $\sim 0.0001$ .

below.

Both the XP and APOGEE samples suggest that only 1 in  $\sim 10^4$  giants within 1 kpc have  $[M/H] < -2.0$ . This very small fraction strongly implies that wide BH companions are overrepresented at low metallicity. If they were not, we could expect to find  $\sim 10^4$  BH companions – just to red giants – within 1 kpc. The true number of BH + giant binaries within 1 kpc is unknown, but 0 have been discovered so far: the nearest such system is Gaia BH2 at  $d = 1.16$  kpc (El-Badry et al. 2023b). It seems quite unlikely that  $10^4$  remain to be discovered (although published *Gaia* data are not yet sensitive to orbital periods as long as that of Gaia BH3), and so a more plausible explanation is that wide BH companions are more common at low metallicity.

#### 4.2. More low-metallicity BHs are expected in DR4

There is also reason to believe that more BHs orbited by metal-poor stars exist in the solar neighborhood. Such stars are uniformly  $\gtrsim 12$  Gyr old. This means that giants sample a narrow mass range of roughly  $(0.78 - 0.80) M_{\odot}$ . For a Kroupa IMF, there are  $\sim 165$  stars with  $M = (0.1 - 0.78) M_{\odot}$  for every star with  $M = (0.78 - 0.80) M_{\odot}$ , suggesting that even within 1 kpc, other massive BHs are likely orbited by lower-mass metal-poor stars that are still on the main sequence. The mass distribution of companions to BHs of course may be different from the IMF, but it seems unlikely that  $0.8 M_{\odot}$  companions would be significantly more common than companions with mass of  $0.7 M_{\odot}$  or  $0.6 M_{\odot}$ . At the distance and extinction of Gaia BH3, such companions

would have  $G < 14$  for  $M > 0.75 M_{\odot}$ , or  $G < 16$  for  $M > 0.61 M_{\odot}$ . These magnitudes are too faint for *Gaia* to have measured multi-epoch RVs from RVS spectra, but bright enough that the astrometric orbit would be resolved with  $\text{SNR} \gtrsim 100$ . With careful processing of the astrometric data, a source like Gaia BH3 could likely be detected even at  $G = 18 - 19$  – where individual astrometric measurements have uncertainties of 1-3 mas in the along-scan direction, a factor of 10-30 smaller than Gaia BH3’s photocenter ellipse (Lindegren et al. 2018) – although spurious solutions will be more abundant at low SNR. Gaia BH3-like systems can thus quite plausibly be detected with significantly lower-mass secondaries, and to larger distances, than Gaia BH3 itself.

Unless Gaia BH3 is a major statistical fluke, these considerations suggest that (a) more massive BHs remain to be discovered around nearby metal-poor stars, and (b) the occurrence rate of BH companions is considerably higher at low metallicity than at solar values.

## 5. DISCUSSION

### 5.1. Formation from an isolated binary

There are at least three straightforward channels to form binaries like Gaia BH3 through isolated binary evolution:

1. The progenitor of the BH could have become a red supergiant but never overflowed its Roche lobe. The MESA models described in Section 3 have maximum radii of  $1000 - 1800 R_{\odot}$ . Meanwhile, Monte Carlo kick simulations (Figure 1) suggest a median pre-SN separation of  $\sim 4500 R_{\odot}$ , such that the BH progenitor would only have overflowed its Roche lobe if its radius exceed  $\sim 3000 R_{\odot}$ . It thus seems quite possible that the BH progenitor and companion star never interacted.
2. The BH progenitor could have overflowed its Roche lobe shortly before core collapse, such that there was no time for the companion star to spiral very far inward. This does not necessarily require fine-tuning: the models predict that at the very low metallicities relevant to Gaia BH3, massive stars spend most of their post-main sequence evolution as blue/yellow supergiants that are too small ( $R \lesssim 100 R_{\odot}$ ) to overflow their Roche lobes for any plausible pre-SN orbit in Gaia BH3. They do eventually expand to become red supergiants, but only in the last  $\lesssim 1000$  years before core collapse (Figure 3). Roche lobe overflow during this phase may not have left enough time for the companion star to spiral inward significantly.
3. The BH could have formed via chemically homogeneous evolution of a  $\sim 35 M_{\odot}$  star with initial rotation rate  $\Omega/\Omega_{\text{crit}} \gtrsim 0.45$ . Such a star would never have become a red supergiant and so would have comfortably fit within its Roche lobe for any possible initial orbit.

Some caution is advisable in interpreting the maximum radii predicted by the MESA models. The radii of red supergiants are sensitive to a variety of uncertain inputs, such as the convective mixing length and

the treatment of overshooting and semiconvection (Chun et al. 2018; Schootemeijer et al. 2019; Goldberg & Bildsten 2020; Klencki et al. 2021). And no one has ever observed a massive star with a metallicity as low as Gaia BH3, so the evolutionary models are untested. However, I emphasize that (a) the modeling choices produce red supergiant temperatures and luminosities in reasonably good agreement with observations of massive stars in the LMC and SMC (e.g. Schootemeijer et al. 2019), which are the lowest-metallicity galaxies current observable with a large population of evolved massive stars, and (b) the radii predicted by these models are not unusually small compared to the predictions of other work (e.g., the references above). The orbit of Gaia BH3 is simply wide, and can accommodate even very large BH progenitors.

### 5.2. Dynamical formation

The fact that Gaia BH3’s orbit is consistent with having formed through isolated binary evolution does not, of course, rule out the possibility that it formed through dynamic interactions in a dense cluster (e.g. Rastello et al. 2023; Di Carlo et al. 2023; Tanikawa et al. 2024b). Indeed, Balbinot et al. (2024) report a likely association between Gaia BH3 and the ED-2 halo stellar stream, which was most likely formed from a low-mass metal-poor star cluster. This makes it quite natural to consider dynamical formation channels, and cluster models tuned to the progenitor of ED-2 will be able predict the population of BH + stellar binaries they should form (e.g. Kremer et al. 2018; Gieles et al. 2021). Association with a cluster does not, however, guarantee that Gaia BH3 formed dynamically: *most* massive stars form in clusters, and clusters contain both primordial and dynamically-formed binaries. The key uncertainties are the initial density and mass of the cluster and how rapidly it dissolved. If Gaia BH3 formed in a cluster, this would require even weaker kicks than implied by Figure 1, because the escape velocity of plausible low-mass clusters is only a few  $\text{km s}^{-1}$ .

Gaia BH3 is just at the separation beyond which BH+star binaries can avoid a common envelope. Irrespective of whether Gaia BH3 in particular formed from an isolated binary, the models presented here imply that isolated binary evolution produces binaries with orbits similar to Gaia BH3 – which is not the case for closer binaries like Gaia BH1 and BH2 – and future *Gaia* data releases are likely to find these binaries.

Constraints on the separation distribution of BH bina-

ries from DR4 will provide some insight into their dominant formation channel. If these systems form mainly by isolated binary evolution, models predict the BH + low mass star period distribution to rise steeply at  $P_{\text{orb}} \gtrsim 10$  yr (e.g. Breivik et al. 2017; Chawla et al. 2022), the period beyond which a significant fraction of binaries will have avoided a common envelope inspiral. For dynamical formation channels, the period distribution will depend on the mass of the clusters in which most systems are formed, but there is little reason to expect a steep increase at  $P_{\text{orb}} \gtrsim 10$  yr. Fortunately, *Gaia* will obtain an 11-year observational baseline, enabling robust orbital constraints at periods up to  $\sim 20$  years, and perhaps even significantly longer (e.g. Andrews et al. 2023).

The metallicity distribution of BH binaries will also help constrain how they formed. The models presented here suggest that isolated binary evolution is more promising at low metallicity, because the compact nature of massive low-metallicity stars means that they can avoid overflowing their Roche lobes and still form BH + low-mass star binaries in the separation range probed by *Gaia* DR4. On the other hand, the vast majority of dense clusters that have contributed stars to the solar neighborhood had metallicities near solar. If dynamical interactions form most wide BH binaries, most systems should likely have metallicities near solar, similar to Gaia BH1 and BH2 (El-Badry et al. 2023a,b). For example, Tanikawa et al. (2024a) predict that the formation efficiency per unit mass of dynamically formed BH + star binaries increases by less than a factor of  $\sim 5$  between  $[M/H] = 0$  and  $[M/H] = -2$ .

We do not know how many other BHs in the pre-release *Gaia* data were *not* published. Because Gaia BH3 has too long of an orbital period to have been accessible in DR3 – and the BH binary period distribution may rise steeply at long periods, where binaries can avoid interaction and a common envelope – population inference is still uncertain. But prospects for constraining this population in the coming years are bright.

### ACKNOWLEDGMENTS

I thank Jim Fuller, Re’em Sari, Jared Goldberg, Thomas Tauris, Hans-Walter Rix, Vedant Chandra, and Rene Andrae for conversations that were influential to this work, and Jakub Klencki for making his MESA inlists publicly available. This research was supported by NSF grant AST-2307232.

### REFERENCES

- Abdurro’uf et al., 2022, *ApJS*, **259**, 35  
 Andrae R., Rix H.-W., Chandra V., 2023, *ApJS*, **267**, 8  
 Andrews J. J., Breivik K., Chawla C., Rodriguez C. L., Chatterjee S., 2023, *ApJ*, **946**, 111  
 Asplund M., Grevesse N., Sauval A. J., Scott P., 2009, *ARA&A*, **47**, 481  
 Balbinot E., et al., 2024, *arXiv e-prints*, p. [arXiv:2404.11604](https://arxiv.org/abs/2404.11604)  
 Blaauw A., 1961, *Bull. Astron. Inst. Netherlands*, **15**, 265  
 Brandt N., Podsiadlowski P., 1995, *MNRAS*, **274**, 461  
 Breivik K., Chatterjee S., Larson S. L., 2017, *ApJ*, **850**, L13  
 Brott I., et al., 2011, *A&A*, **530**, A115  
 Chawla C., Chatterjee S., Breivik K., Moorthy C. K., Andrews J. J., Sanderson R. E., 2022, *ApJ*, **931**, 107  
 Chun S.-H., Yoon S.-C., Jung M.-K., Kim D. U., Kim J., 2018, *ApJ*, **853**, 79  
 Di Carlo U. N., Agrawal P., Rodriguez C. L., Breivik K., 2023, *arXiv e-prints*, p. [arXiv:2306.13121](https://arxiv.org/abs/2306.13121)  
 Eggleton P. P., 1983, *ApJ*, **268**, 368  
 El-Badry K., et al., 2023a, *MNRAS*, **518**, 1057  
 El-Badry K., et al., 2023b, *MNRAS*, **521**, 4323  
 El-Badry K., et al., 2024, *arXiv e-prints*, p. [arXiv:2402.06722](https://arxiv.org/abs/2402.06722)  
 Fernández R., Quataert E., Kashiyama K., Coughlin E. R., 2018, *MNRAS*, **476**, 2366  
 Gaia Collaboration et al., 2024, *arXiv e-prints*, p. [arXiv:2404.10486](https://arxiv.org/abs/2404.10486)  
 Gieles M., Erkal D., Antonini F., Balbinot E., Peñarrubia J., 2021, *Nature Astronomy*, **5**, 957  
 Goldberg J. A., Bildsten L., 2020, *ApJ*, **895**, L45  
 Hamann W. R., Koesterke L., Wessolowski U., 1995, *A&A*, **299**, 151  
 Heger A., Langer N., Woosley S. E., 2000, *ApJ*, **528**, 368  
 Henyey L., Vardya M. S., Bodenheimer P., 1965, *ApJ*, **142**, 841  
 Jermyn A. S., et al., 2023, *ApJS*, **265**, 15  
 Klencki J., Nelemans G., Istrate A. G., Pols O., 2020, *A&A*, **638**, A55  
 Klencki J., Nelemans G., Istrate A. G., Chruslinska M., 2021, *A&A*, **645**, A54

- Kremer K., Ye C. S., Chatterjee S., Rodriguez C. L., Rasio F. A., 2018, [ApJ](#), **855**, L15
- Langer N., Fricke K. J., Sugimoto D., 1983, *A&A*, **126**, 207
- Lindgren L., et al., 2018, *A&A*, **616**, A2
- Maeder A., 1987, *A&A*, **178**, 159
- Majewski S. R., et al., 2017, *AJ*, **154**, 94
- Nieuwenhuijzen H., de Jager C., 1990, *A&A*, **231**, 134
- O'Connor C. E., Bildsten L., Cantiello M., Lai D., 2023, *ApJ*, **950**, 128
- Paxton B., Bildsten L., Dotter A., Herwig F., Lesaffre P., Timmes F., 2011, *ApJS*, **192**, 3
- Paxton B., et al., 2013, *ApJS*, **208**, 4
- Paxton B., et al., 2015, *ApJS*, **220**, 15
- Paxton B., et al., 2018, *ApJS*, **234**, 34
- Paxton B., et al., 2019, *ApJS*, **243**, 10
- Rastello S., Iorio G., Mapelli M., Arca-Sedda M., Di Carlo U. N., Escobar G. J., Shenar T., Torniamenti S., 2023, *MNRAS*, **526**, 740
- Schootemeijer A., Langer N., Grin N. J., Wang C., 2019, *A&A*, **625**, A132
- Tanikawa A., Wang L., Fujii M. S., 2024a, [arXiv e-prints](#), p. [arXiv:2404.01731](#)
- Tanikawa A., Cary S., Shikauchi M., Wang L., Fujii M. S., 2024b, *MNRAS*, **527**, 4031
- Tauris T. M., van den Heuvel E. P. J., 2023, *Physics of Binary Star Evolution. From Stars to X-ray Binaries and Gravitational Wave Sources*, [doi:10.48550/arXiv.2305.09388](#).
- Tauris T. M., et al., 2017, *ApJ*, **846**, 170
- Vink J. S., de Koter A., Lamers H. J. G. L. M., 2000, *A&A*, **362**, 295
- Vink J. S., de Koter A., Lamers H. J. G. L. M., 2001, *A&A*, **369**, 574
- Woosley S. E., Heger A., 2006, *ApJ*, **637**, 914
- Woosley S. E., Heger A., Weaver T. A., 2002, *Reviews of Modern Physics*, **74**, 1015
- Yoon S. C., Langer N., 2005, *A&A*, **443**, 643
- Yoon S. C., Langer N., Norman C., 2006, *A&A*, **460**, 199

This paper was built using the Open Journal of Astrophysics L<sup>A</sup>T<sub>E</sub>X template. The OJA is a journal which

provides fast and easy peer review for new papers in the **astro-ph** section of the arXiv, making the reviewing process simpler for authors and referees alike. Learn more at <http://astro.theoj.org>.